UC Berkeley

UC Berkeley Previously Published Works

Title

Determination of the Exchange Current Density With Polymer Electrolytes and Its Correlation With Coulombic Efficiency

Permalink

https://escholarship.org/uc/item/5z69104t

Journal

Small Structures, 7(7)

ISSN

2688-4062

Authors

Geng, Katrin

Espinosa-Angeles, Julio C

Patel, Vivaan

et al.

Publication Date

2026-07-01

DOI

10.1002/sstr.70532

Copyright Information

This work is made available under the terms of a Creative Commons Attribution License, available at https://creativecommons.org/licenses/by/4.0/

Peer reviewed

eScholarship.org Powered by the California Digital Library
University of California

Small Structures

small structures

www.small-structures.com

RESEARCH ARTICLE OPEN ACCESS

Determination of the Exchange Current Density With Polymer Electrolytes and Its Correlation With Coulombic Efficiency

Katrin Geng[1,2] | Julio C. Espinosa-Angeles[1,2] | Vivaan Patel[3,4] | Ziyuan Lyu[1,2] | Bryce A. Tappan[5] | Nitash Balsara[3,4] | Stefano Passerini[1,2,6] | Yang Shao-Horn[5,7,8] | Dominic Bresser[1,2,9]

[1]Helmholtz Institute Ulm (HIU), Ulm, Germany | [2]Karlsruhe Institute of Technology (KIT), Karlsruhe, Germany | [3]Department of Chemical and Biomolecular Engineering, University of California, Berkeley, Berkeley, California, USA | [4]Materials Sciences Division, Lawrence Berkeley National Laboratory, Berkeley, California, USA | [5]Research Laboratory of Electronics, Massachusetts Institute of Technology (MIT), Cambridge, Massachusetts, USA | [6]Center for Transportation Technologies, Austrian Institute of Technology (AIT), Vienna, Austria | [7]Department of Materials Science and Engineering, Massachusetts Institute of Technology (MIT), Cambridge, Massachusetts, USA | [8]Department of Mechanical Engineering, Massachusetts Institute of Technology (MIT), Cambridge, Massachusetts, USA | [9]Ulm University (UUlm), Ulm, Germany

Correspondence: Yang Shao-Horn (shaohorn@mit.edu) | Dominic Bresser (dominic.bresser@kit.edu)

Received: 27 January 2026 | **Revised:** 19 June 2026 | **Accepted:** 24 June 2026

Keywords: battery | Coulombic efficiency | exchange current density | lithium metal | polyethylene oxide | polymer electrolyte

ABSTRACT

Polymer electrolytes are promising materials to enable practical lithium-metal batteries for high-energy-density energy storage. Yet, parasitic side reactions at the lithium|polymer interface and inhomogeneous lithium deposition, compromising cycling reversibility and safety, remain a challenge. Despite the key role of the interfacial reactivity, there is a lack of quantitative and comparable information on interfacial charge–transfer kinetics with polymer electrolytes, and their impact on the lithium plating/stripping behavior remains unclear. Therefore, in this work, we apply a validated method for quantifying interfacial charge–transfer kinetics via the exchange current density j_0 to a series of polyethylene oxide (PEO)-based polymer electrolytes to clarify how the electrolyte composition influences interfacial kinetics. By combining the j_0 analyses with measurements of the solid electrolyte interphase resistance and lithium cycling reversibility, we identify a consistent trend in which smaller j_0 and higher R_{SEI} values correlate with higher Coulombic efficiencies. This indicates that moderated interfacial kinetics and a sufficiently passivating interphase favor higher plating/stripping reversibility. The results provide a coherent dataset of interfacial charge–transfer parameters for polymer electrolytes and highlight the importance of deliberate electrolyte and interphase design for achieving highly reversible lithium-metal cycling in polymer-based electrolyte systems.

1 | Introduction

Lithium-metal batteries (LMBs) with polymer electrolytes, often incorporating certain amounts of a liquid phase to boost the ionic conductivity, are receiving a lot of attention as promising candidates for next-generation high-energy density storage systems [1, 2]. Despite their great potential, though, the reactivity at the lithium|polymer interface is still insufficiently understood. A key descriptor for the interfacial charge transfer reactivity is the exchange current density, j_0, which quantifies the magnitude of the forward and reverse rate of charge transfer under equilibrium conditions. Beyond its classical role in the Butler–Volmer framework, the exchange current density is also connected to the electrodeposition process through its influence on the nucleation overpotential and the associated Gibbs energy barrier, linking interfacial kinetics to the lithium morphology evolution [3].

This is an open access article under the terms of the Creative Commons Attribution License, which permits use, distribution and reproduction in any medium, provided the original work is properly cited.

© 2026 The Author(s). *Small Structures* published by Wiley-VCH GmbH.

Recent works on liquid electrolytes have hypothesized that j_0 can govern the coupling between interfacial charge–transfer kinetics and ion transport, and can therefore impact the Coulombic efficiency (CE) (i.e., the reversibility of the lithium stripping and plating process) by modulating the homogeneity of the local current distribution and, thereby, the lithium deposition morphology [4–6]. Since the CE directly determines the long-term cyclability and practical viability of LMBs, identifying the fundamental parameters that govern the CE is of central importance for the rational design of advanced electrolyte systems. In this context, understanding whether and how the exchange current density influences the CE represents a key step toward linking interfacial kinetics to battery performance metrics.

While the aforementioned studies [4–6] underscore the relevance of j_0 for understanding and improving the reversibility in LMB systems, easy-to-compare, reliable j_0 values for polymer electrolytes remain scarce. The reported values vary widely, in part due to the use of inconsistent measurement and analysis approaches [7]. For example, the often overlooked influence of the solid electrolyte interphase (SEI) layer can significantly affect the measured values, complicating a direct comparison and a meaningful interpretation [7]. Moreover, the connection between interfacial charge–transfer kinetics and CE has – to the best of our knowledge – not yet been systematically investigated for polymer electrolyte systems. Establishing such a relationship would clarify whether j_0 can serve as a meaningful descriptor linking electrolyte composition, interfacial kinetics, and the reversibility of the lithium plating and stripping process. This gap is particularly critical given competing hypotheses: a higher j_0 might facilitate a faster charge transfer and improve the plating/stripping process, but could also accelerate reductive electrolyte decomposition and SEI growth, resulting in a reduced CE. On the other hand, a lower j_0 might promote a more homogeneous current distribution and smooth lithium deposition, in turn resulting in higher CE. Consequently, a systematic investigation of the correlation between j_0 and CE is required to determine whether and how interfacial charge–transfer kinetics govern the reversibility of lithium metal electrodes in combination with polymer electrolytes.

In this study, we address these open questions by applying a previously validated and consistent methodology for determining the exchange current density [7] to a broad set of PEO-based (gel) polymer electrolytes containing different conducting salts and liquid plasticizers. We chose PEO-based systems, since they represent the most extensively studied polymer electrolyte platform and therefore provide an ideal model system for a systematic investigation of the interfacial kinetics. This systematic approach enables the direct comparison of j_0 values across different electrolyte compositions and provides new insights into the question of how the polymer electrolyte composition influences interfacial charge–transfer kinetics. Building on this comprehensive data set, we further investigate whether j_0 and the related SEI resistance correlate with the CE of the lithium plating and stripping process, thereby evaluating how interfacial kinetics govern lithium reversibility in polymer-based LMBs and providing guidance for the rational design of advanced polymer electrolytes.

2 | Results and Discussion

2.1 | Influence of the Polymer Composition on the Exchange Current Density

The exchange current density j_0 was determined for a set of eleven different PEO-based electrolyte systems containing four different conducting salts, lithium bis(trifluoromethanesulfonyl)imide (LiTFSI), lithium (fluorosulfonyl)(trifluoromethanesulfonyl)imide (LiFTFSI), lithium perchlorate ($LiClO_4$), and lithium bis(fluorosulfonyl)imide (LiFSI) – with and without a liquid plasticizer – as well as one block-copolymer polystyrene-*b*-poly(ethylene oxide) (PS-PEO). The plasticizers employed were the ionic liquids 1-butyl-1-methylpyrrolidinium bis(trifluoromethanesulfonyl)imide ($Pyr_{14}TFSI$) and 1-butyl-1-methylpyrrolidinium (fluorosulfonyl)(trifluoromethanesulfonyl)imide ($Pyr_{14}FTFSI$), as well as tetraethylene glycol dimethyl ether (TEGDME).

To determine j_0 for these materials, we applied a method previously established and validated on PEO-based polymer electrolytes for LMBs to ensure comparability [7], which is essential for assessing how the polymer electrolyte composition influences j_0. Accordingly, symmetric Li||Li cells were assembled and allowed to rest at open-circuit voltage for 24 h before conducting electrochemical impedance spectroscopy (EIS) in a first step. By fitting the EIS results (displayed as Nyquist plots) with a suitable equivalent circuit model, the charge transfer resistance (R_{ct}) can be extracted (see Figure 1) [7]. Alternatively, distribution of

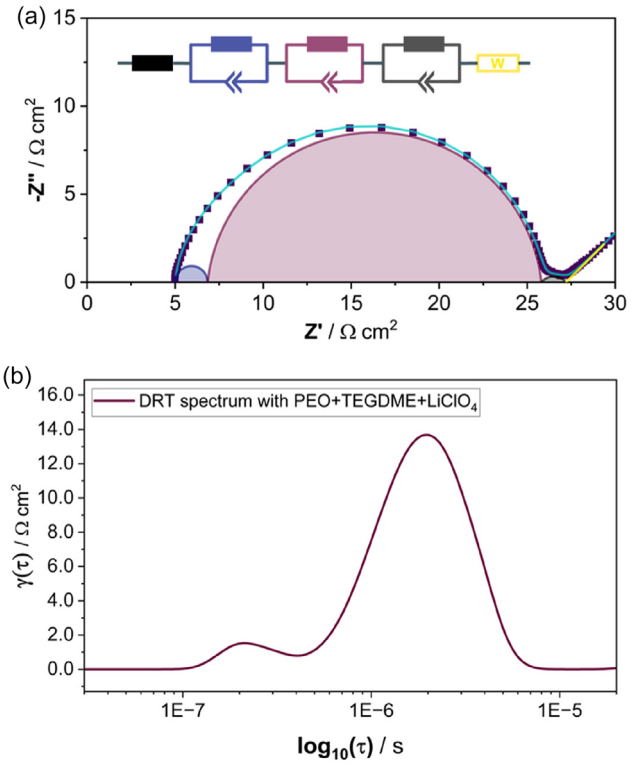


FIGURE 1 | Exemplary EIS results for a Li||Li cell with PEO, TEGDME, and $LiClO_4$, measured at 80 °C. (a) Nyquist plot with equivalent circuit model fit, (b) Distribution of relaxation times analysis in the mid frequency region between 10^{-8} and 10^{-5} s. The feature at higher frequencies corresponds to the charge transfer resistance.

26884062, 2026, 7, Downloaded from https://onlinelibrary.wiley.com/doi/10.1002/sstr.70532, Wiley Online Library on [17/11/2026]. See the Terms and Conditions (https://onlinelibrary.wiley.com/terms-and-conditions) on Wiley Online Library for rules of use; OA articles are governed by the applicable Creative Commons License

relaxation times (DRT) analysis, which transforms the frequency-dependent impedance spectrum into the time domain so that the polarization contributions appear as distinct peaks, allows for the extraction of R_{ct} via Gaussian peak fitting [7]. The exchange current density is directly related to the charge transfer resistance via the Butler–Volmer equation, which simplifies to Equation (1):

$$j_0 = \mathrm{RT}/n\mathrm{FR}_{ct} \quad (1)$$

for small overpotentials, where R is the ideal gas constant, T is the temperature in Kelvin, n is the number of electrons transferred, and F is the Faraday constant.

The results for j_0 obtained using these methods are shown in Figure 2. As evident from Figure 2a (40 °C) and Figure 2b (80 °C), the values derived from Nyquist plot fitting and DRT analysis are in very good agreement and consistent with previous findings [7]. Therefore, in the remainder of this manuscript, we present the j_0 values obtained from Nyquist plot fitting. These j_0 values are also compiled in Table 1.

In general, the determined j_0 values fall within the expected range for PEO-based electrolytes at elevated temperatures. For instance, j_0 of PEO + LiTFSI at 40 °C aligns well with what has been reported in the literature [7, 8]. A comparison of the scales in Figure 2a,b clearly illustrates a temperature dependence of the exchange current density: j_0 increases by approximately one order of magnitude from 40 °C to 80 °C for all polymer compositions. This trend is consistent with the thermally activated nature of the interfacial kinetics, described by the Arrhenius equation:

$$j_0 \sim e^{-\frac{E_a}{RT}} \quad (2)$$

where E_a is the activation energy for the charge transfer process. With only two data points per material (at 40 °C and 80 °C), and considering that PEO melts at around 65 °C (which affects the slope of the Arrhenius plot) [9], the activation energies can only be roughly estimated. "$E_a(R_{ct})$" and "$E_a(R_{SEI})$" range from 46 to 60 kJ mol^{-1}, corresponding to 0.48–0.66 eV. On average, j_0 increased by a factor of 13 ± 7 from 40 °C to 80 °C. To contextualize these results, we compare them with values reported in the literature. Egashira et al. [10] reported charge transfer activation energies between 25 kJ mol^{-1} (at 60 °C–70 °C) and 69 kJ mol^{-1} (at 35 °C–60 °C) for PEO with $LiBF_4$, agreeing well with our findings. Isaac et al. [11] found the activation energy for charge transfer at Li|PEO + LiTFSI interfaces to be 0.72 ± 0.03 eV between 70 °C and 100 °C, slightly higher than our estimate. We also compared the increase in j_0 from 40 °C to 80 °C in previous studies. These values –16 for PEO + $LiCF_3SO_3$ [12], 14.5 with PEO + LiI [12], and 6 for PEO + $LiBF_4$ [10] – are consistent with our observation (13 ± 7).

We further show that temperature has the most significant impact, although also the polymer composition (such as modifying the matrix from PEO to PS-PEO, the salt, and the addition of a plasticizer) influences j_0. This becomes evident by plotting the

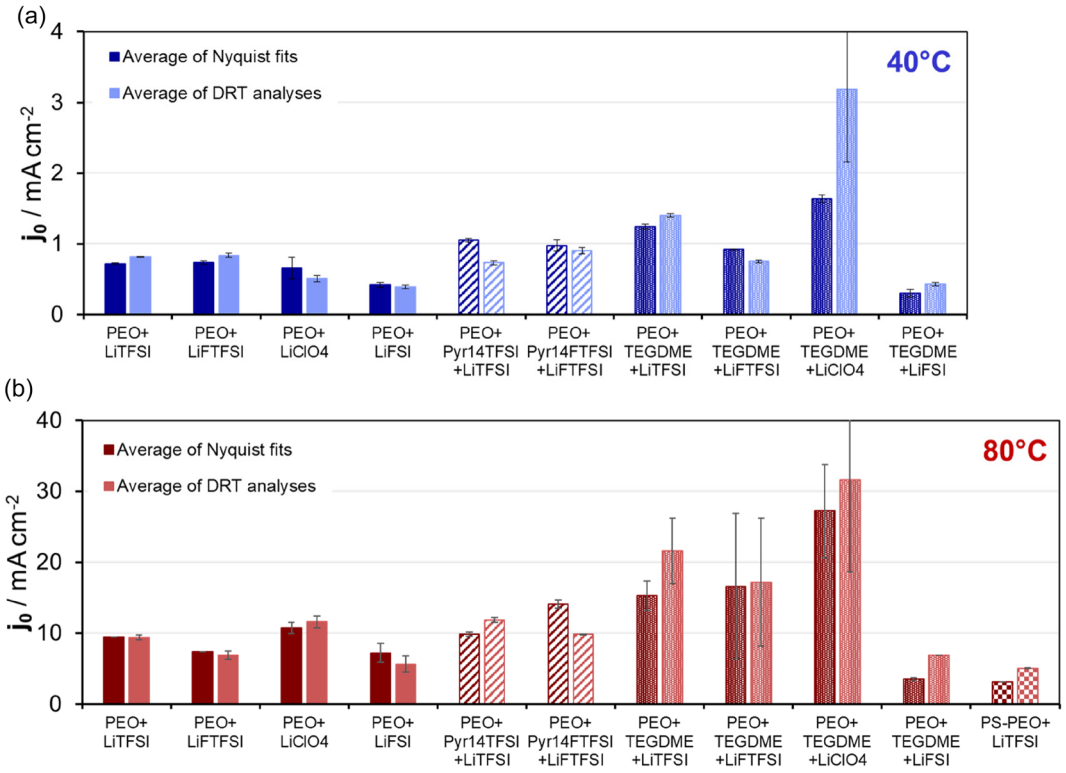


FIGURE 2 | Comparison of the exchange current densities j_0 determined by EIS for different PEO-based polymer electrolyte compositions in Li||Li cells. The EIS data measured at (a) 40 °C and (b) 80 °C were analyzed by Nyquist plot fitting (dark color) and DRT analysis (bright color) to extract j_0. The j_0 values were multiplied by two to represent per-interface values. The polymer electrolytes contained four different salts (monochrome), an ionic liquid as plasticizer (striped), TEGDME as plasticizer (spotted), and/or a different polymer matrix (checkered).

26884062, 2026, 7, Downloaded from https://onlinelibrary.wiley.com/doi/10.1002/sstr.70532, Wiley Online Library on [17/11/2026]. See the Terms and Conditions (https://onlinelibrary.wiley.com/terms-and-conditions) on Wiley Online Library for rules of use; OA articles are governed by the applicable Creative Commons License

TABLE 1 | Exchange current densities j_0 determined by Nyquist plot fitting of EIS data for different PEO-based polymer electrolyte compositions in Li‖Li cells.

	PEO + LiTFSI	PEO + LiFTFSI	PEO + $LiClO_4$	PEO + LiFSI	PEO + TEGDME + LiTFSI	PEO + TEGDME + LiFTFSI	PEO + TEGDME + $LiClO_4$	PEO + TEGDME + LiFSI	PEO + $Pyr_{14}TFSI$ + LiTFSI	PEO + $Pyr_{14}FTFSI$ + LiFTFSI	PS-PEO + LiTFSI
j_0, 40 °C/mA cm^{-2}	0.72 ± 0.01	0.74 ± 0.02	0.66 ± 0.15	0.42 ± 0.04	1.24 ± 0.04	0.92 ± 0.01	1.64 ± 0.06	0.30 ± 0.05	1.06 ± 0.03	0.98 ± 0.08	—
j_0, 80 °C/mA cm^{-2}	9.44 ± 0.04	7.40 ± 0.01	10.69 ± 0.78	7.21 ± 1.37	15.25 ± 2.06	16.60 ± 10.25	27.22 ± 6.58	3.54 ± 0.18	9.83 ± 0.27	14.09 ± 0.63	3.10 ± 0.03

Note: The EIS data were measured at 40 °C and 80 °C. The j_0 values were multiplied by two to represent per-interface values.

exchange current densities grouped by the comprised lithium salt, as shown in Figure 3. Generally, the exchange current density increases with the addition of an ionic liquid ($Pyr_{14}TFSI$ or $Pyr_{14}FTFSI$) and further increases with the incorporation of TEGDME as an alternative plasticizer (except for LiFSI, for which it decreases slightly when adding TEGDME). This trend is especially evident in the inset of Figure 3a PEO + LiTFSI at 40 °C and in Figure 3c (PEO + $LiClO_4$ at both 40 °C and 80 °C), which can be attributed to altered lithium solvation environments associated with the plasticization of polymer electrolytes. First, the presence of liquid components enhances the ionic conductivity and mobility due to: (i) increased amorphicity [13], which is essential since ion transport in PEO-based electrolytes predominantly occurs in the amorphous phase (ii) increased "free volume" available for the charge transport which facilitates ion hopping between coordination sites since the space facilitates polymer chain movement [14], and therefore (iii) improved dynamics of the polymer chain segments [15], all promoting more efficient lithium-ion transfer to the reaction interface. In addition, liquid plasticizers can increase interfacial wetting and contact [16], to provide higher dielectric environments [17], and beneficially modify the solvation environment of lithium ions [18], which can reduce the energy barrier for the lithium-ion transfer and facilitate the charge transfer step.

Contrary to the effect of introducing a plasticizer, the modification of the polymer matrix from PEO to PS-PEO led to a lower exchange current density (Figure 2b). This may be explained by the more rigid nature of the PS-PEO block copolymer [19], resulting in hampered chain reorganization during the charge transfer step, thus causing a higher charge transfer resistance and, hence, a lower j_0.

In addition to the plasticizer and the polymer matrix, the nature of the conducting salt also has a non-negligible influence on j_0, which has been observed previously for liquid electrolytes as well [4]. For example, we found similar exchange current densities for electrolytes with LiTFSI and LiFTFSI, which are higher than those obtained for $LiClO_4$, but lower than those found for LiFSI. Different anions in the salt can alter salt association energetics [20], and ion-pair formation tendencies [21], which can modify lithium-ion coordination structures and influence desolvation and charge transfer kinetics [18, 20, 22, 23]. While salts have been reported to influence the composition of the SEI and the apparent j_0, we decouple these effects in this work, considering j_0 independently of the SEI resistance.

We further compare the j_0 values of polymer electrolytes in this study with previous work, where the scope is limited due to the scarcity of reported j_0 or R_{ct} values. The j_0 value for PEO + LiTFSI at 40 °C (0.72 ± 0.01 mA cm^{-2}) aligns well with previously reported results (0.75 ± 0.05 mA [7], 0.7 ± 0.1 mA cm^{-2} [8]). In addition, Wetjen et al. [24] reported j_0 values of 0.06 mA cm^{-2} at 40 °C and 0.25 mA cm^{-2} at 80 °C for PEO-containing $Pyr_{14}TFSI$, which are lower than our findings. However, their measurements did not account for the SEI resistance, unlike this work, which might be responsible for lower j_0 values. Moreover, Appetecchi et al. [25] reported a charge transfer resistance corresponding to an exchange current density of $j_0 = 0.41$ mA cm^{-2} for a polymeric ionic liquid with $Pyr_{14}TFSI$ and LiTFSI at 40 °C after 30 days of rest, which, considering the different polymer matrix, is in

26884062, 2026, 7, Downloaded from https://onlinelibrary.wiley.com/doi/10.1002/sstr.70532, Wiley Online Library on [17/11/2026]. See the Terms and Conditions (https://onlinelibrary.wiley.com/terms-and-conditions) on Wiley Online Library for rules of use; OA articles are governed by the applicable Creative Commons License

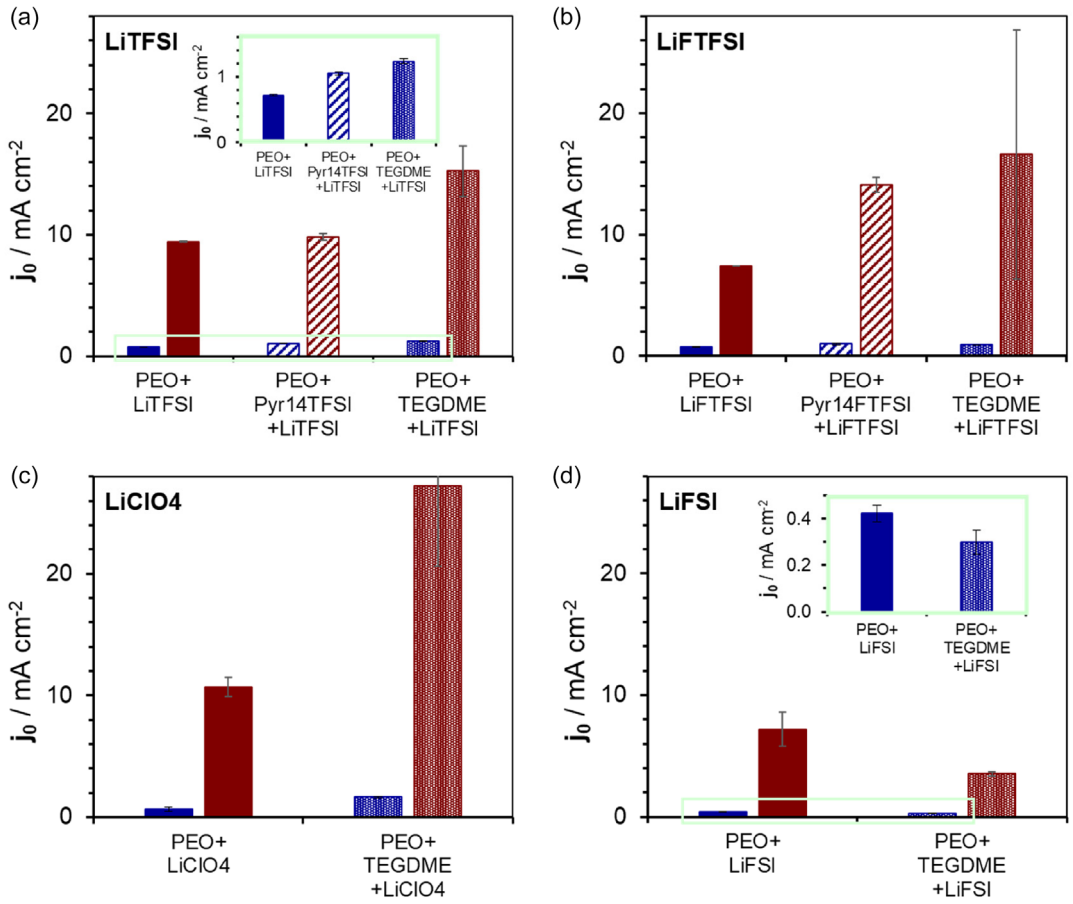


FIGURE 3 | Exchange current densities j_0 determined by EIS for different PEO-based polymer electrolyte compositions in Li||Li cells at 40 °C (blue) and 80 °C (red). Panels (a–d) show the j_0 results from Nyquist plot fitting (see Figure 1) grouped by the containing conducting salt, being (a) LiTFSI, (b) LiFTFSI, (c) $LiClO_4$, and (d) LiFSI.

reasonable agreement with our finding of ~0.7 mA cm^{-2}. Lastly, Munichandraiah et al. [26] provided R_{ct} values for PEO + $LiClO_4$ from EIS measurements, which can be translated to $j_0 = 0.24$ mA cm^{-2} at 80 °C. While this value is smaller than ours (0.72 ± 0.01 mA cm^{-2}), a twofold increase in j_0 when plasticizing the PEO + $LiClO_4$ electrolyte with propylene carbonate agrees well with our observations when plasticizing with TEGDME (Figure 3).

Overall, these results demonstrate that the exchange current density at the lithium|polymer interface is strongly governed by the electrolyte composition – particularly the polymer matrix, plasticization, and salt chemistry – and that the consistently determined j_0 values are in good agreement with literature reports when differences in methodology and SEI contributions are accounted for. Having established a coherent and comparable dataset of interfacial charge–transfer kinetics for these polymer electrolytes, we now turn to examining how the magnitude of j_0 relates to the reversibility of lithium plating and stripping, as quantified by the CE.

2.2 | Correlation of the Exchange Current Density With the CE

Having consistently determined the exchange current densities for a set of different polymer electrolytes, the question of how j_0 relates to the lithium plating/stripping reversibility is addressed next. To assess the influence of j_0 on the plating/stripping behavior, the average CEs were determined over ten cycles (following a formation cycle) in Cu||Li cells using the method described by Adams et al. [27]. Figure 4 shows the relationship between j_0 and the average CE at 40 °C (Figure 4a) and at 80 °C (Figure 4b). Although the determination of the CE could not be performed at 40 °C for some materials (namely, PEO + $LiClO_4$, PEO + LiFSI, and PS-PEO+LiTFSI) due to experimental limitations (e.g., poor ionic conductivity at such a temperature) [28–30], the remaining data points reveal a general trend of an increasing CE with a decreasing j_0. For the data at 40 °C in Figure 4a, this is graphically illustrated by the ellipse and statistically evident from the negative Pearson correlation coefficient (PPC) of −0.68. While a PPC of 0 would indicate no linear correlation between the variables, a value of −1 or 1 would indicate a perfect linear relationship, with all data points lying on a straight line with a negative or positive slope, respectively. Although the trend is less pronounced at 80 °C (Figure 4b), also because of a generally lower CE, a subtle correlation between higher CE and lower j_0 with a PPC of −0.22 is still observed. Hence, also at 80 °C, a higher CE coincides with lower j_0 values. Nonetheless, at such elevated temperatures the electrolyte decomposition kinetics get faster as well, potentially impacting the CE too – not least owing to an increased polymer flowability above the melting temperature (which lies between the two measurement temperatures) [31]. The easier transport of

26884062, 2026, 7, Downloaded from https://onlinelibrary.wiley.com/doi/10.1002/sstr.70532, Wiley Online Library on [17/11/2026]. See the Terms and Conditions (https://onlinelibrary.wiley.com/terms-and-conditions) on Wiley Online Library for rules of use; OA articles are governed by the applicable Creative Commons License

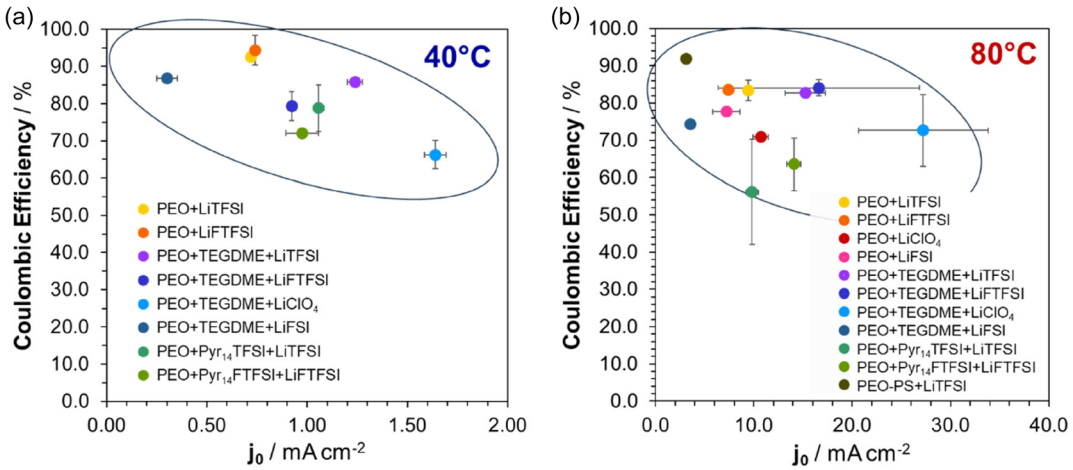


FIGURE 4 | Correlation of exchange current density j_0 with CE. The j_0 values obtained at (a) 40 °C and (b) 80 °C for a set of PEO-based polymer electrolytes with different composition (see Figures 2 and 3) are plotted versus the respective average CEs determined in Cu||Li cells. The PCC for these data points is −0.68 at 40 °C and −0.22 at 80 °C.

reactive species to the lithium|electrolyte interface further facilitates parasitic side reactions, reducing the CE [32]. Another factor potentially impacting the CE is the reduction in mechanical strength due to thermal softening [33, 34], which is particularly pronounced for the initially robust nonplasticized polymer electrolytes such as PEO + LiTFSI and PEO + LiFTFSI (because plasticized electrolytes already show much lower mechanical moduli at low temperature, see Figure S1a) [35]. The dry materials, in fact, experience a relatively greater decrease in CE from 40 °C to 80 °C. As shown by Monroe and Newman [36] and our recent work [35], mechanically stiff solid polymer electrolytes promote a more compact lithium deposition, which mitigates lithium losses associated with electrically isolated "dead" lithium during stripping and increases the CE. This hypothesis may be supported by the observation of PS-PEO + LiTFSI, which exhibits a higher CE than the other materials (Figure 4b). While it shows the lowest j_0, consistent with the general trend we observed (i.e., smaller j_0 corresponds to higher CE), its elevated CE may also be partially attributed to the increased mechanical stiffness of the block-copolymer matrix (compare Figure S1b) [37].

To facilitate the comparison with the previously reported analysis with liquid electrolytes by Hobold et al. [4], Figure 5 presents the data from Figure 4 plotted as CE versus j/j_0 (instead of j_0) on a logarithmic x-axis. Hobold et al. [4] reported that the CE initially increases with increasing j/j_0, reaches a maximum at around 10 j/j_0, and subsequently decreases. In the present study, the accessible range is limited to $j/j_0 < 1$, as a further uniform increase in current density j was experimentally not feasible due to the limited conductivity of some materials, particularly at 40 °C [28, 29]. As shown in Figure 5, within this accessible regime, a similar trend is observed, as the CE tends to increase with increasing j/j_0, (i.e., decreasing j_0). Hobold et al. [4] proposed that a lower j_0 can lead to a more uniform current distribution for plating, resulting in a higher CE. Nonetheless, the studies used for their analysis did not account for the SEI when determining j_0 by linear fitting of the Tafel plots [3, 38]. Consequently, their reported j_0 values may be generally lower due to the contribution of the SEI resistance (R_{SEI}), leaving space for an alternative interpretation: a low apparent j_0 may reflect a passivating, homogeneous, and resistive SEI that suppresses further electrolyte decomposition, thus contributing to higher CEs. To test this hypothesis, we

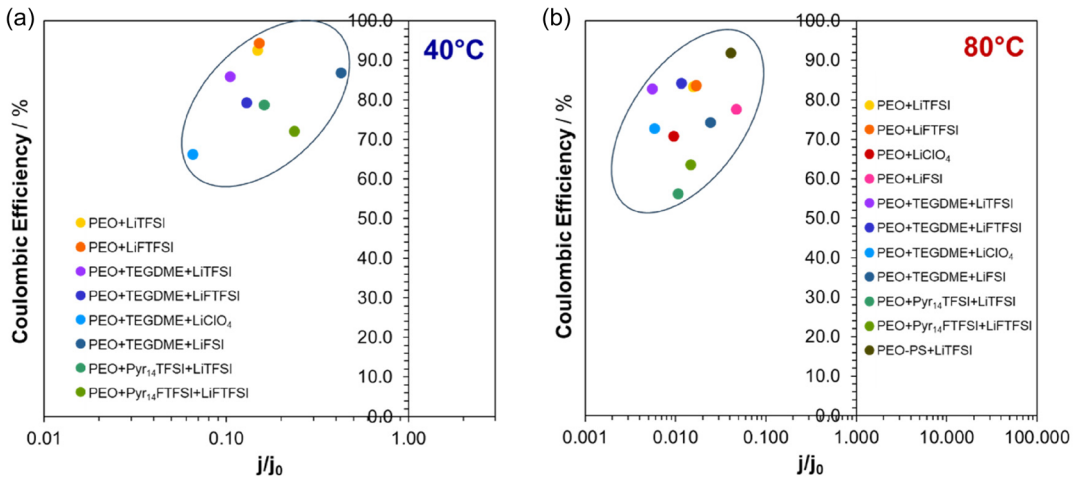


FIGURE 5 | Correlation of the CE with j/j_0, where j is the current density applied during the CE determination and j_0 the exchange current density. Data are presented for a set of PEO-based polymer electrolytes with different compositions at (a) 40 °C and (b) 80 °C.

26884062, 2026, 7, Downloaded from https://onlinelibrary.wiley.com/doi/10.1002/sstr.70532, Wiley Online Library on [17/11/2026]. See the Terms and Conditions (https://onlinelibrary.wiley.com/terms-and-conditions) on Wiley Online Library for rules of use; OA articles are governed by the applicable Creative Commons License

first extracted the R_{SEI} values from the EIS and DRT data (similar to the R_{ct} determination), as displayed in Figure 6. Similar to the j_0 data in Figure 2, good agreement between Nyquist plot fitting and DRT analysis was obtained. Using these values, we examined the relationship between R_{SEI} and CE, as shown in Figure 7. As highlighted by the ellipses and evident from the PPC ≠ 0 (0.18 at 40 °C and 0.35 at 80 °C), a higher R_{SEI} does indeed appear to correlate with a larger CE at both temperatures. This correlation between R_{SEI} and CE is indicative of the formation of a passivating, homogeneous, and resistive SEI.

Thus, we find a discernible correlation between both R_{ct} ($\sim 1/j_0$) and R_{SEI} with CE, revealing the trend that higher interfacial resistances (both R_{ct} and R_{SEI}) relate to higher CEs across the studied polymer electrolytes. Since the magnitude of R_{ct} and R_{SEI} correlates linearly, as evident from Figure 8, their individual influence on CE remains difficult to isolate. Nonetheless, the data suggest that both resistances are connected to reversibility, even though potentially in ways that depend on additional factors.

Several parameters could contribute to the imperfect correlation. Studies on liquid electrolytes suggest that at lower CE values, dead lithium formation dominates, while at higher CEs, SEI transport and lithium-ion charge transfer properties become key differentiators [4]. If similar mechanisms apply to polymer-based electrolytes, the influence of j_0 may become more pronounced in materials that already achieve very high CE. Additionally, differences in mechanical properties – such as stiffness and modulus – were not included in this analysis, but are known to affect the lithium morphology and, thus, also the CE [35, 36].

Despite these complexities, the observed trends are consistent with established mechanistic models: a lower j_0 leads to a higher critical nucleus size and supports a more uniform current distribution at the lithium interface [3, 4]. Both effects are conducive to denser, more uniform lithium growth and improved cycling stability [3, 39]. Additionally, a homogeneous and passivating SEI further contributes to smooth lithium plating and stripping, while limiting the progression of parasitic side reactions with the electrolyte [39]. Thus, while fast charge–transfer kinetics are generally considered favorable to achieve high rate capability, this study highlights that in polymer-based systems, slower interfacial kinetics – associated with higher interfacial resistances – can be beneficial for promoting more favorable lithium deposition and higher reversibility.

It should be noted, however, that this observation does not imply that j_0 should be minimized unconditionally. In PEO-based solid polymer electrolytes, the accessible current density is primarily constrained by the limiting current density, which is governed by ionic conductivity, transference number, and electrolyte thickness, rather than by j_0 alone [40, 41]. Within the operating window typical of practical polymer-based LMBs (C/10–C/3) [42], moderately slow charge–transfer kinetics can act as a stabilizing factor by suppressing local current inhomogeneities and promoting more uniform nucleation and growth of lithium [3, 43], while not necessarily constituting the dominant rate-limiting step for power delivery under these conditions [40, 44]. The practical design challenge is therefore to co-optimize j_0 and the properties of the SEI such that the lithium deposition remains uniform and kinetically moderated at the target current density [43], while ensuring that the overall interfacial resistance does not excessively compromise rate capability [41].

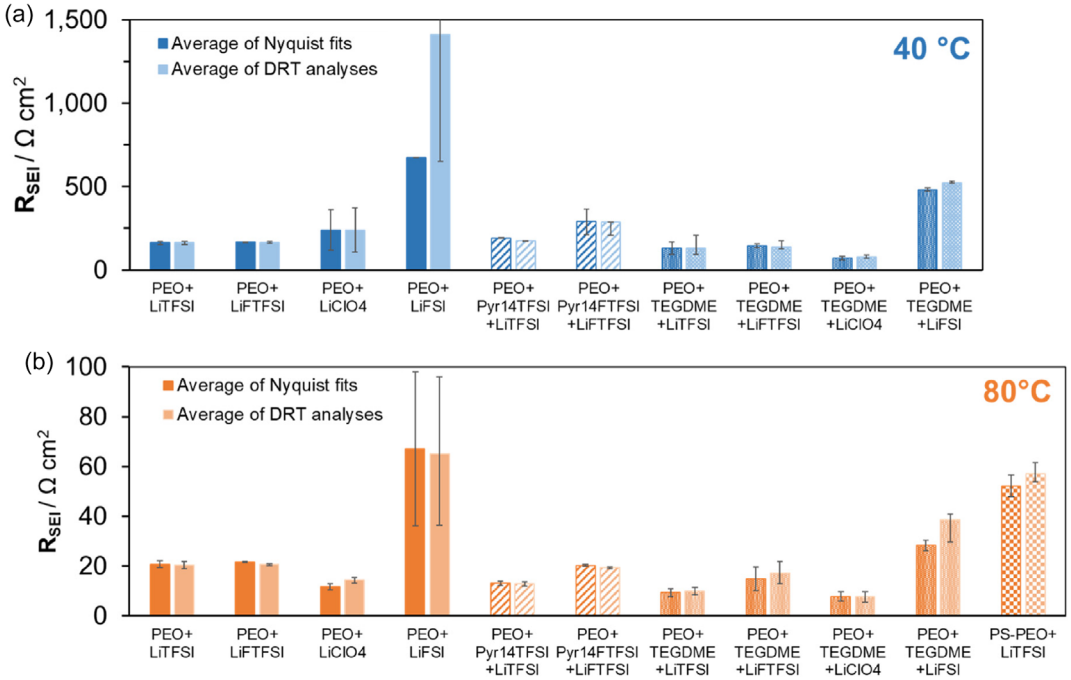


FIGURE 6 | SEI resistance R_{SEI} determined by EIS for different PEO-based polymer electrolyte compositions in Li||Li cells. The polymer electrolytes contained four different salts (monochrome), ionic liquid as plasticizer (striped), TEGDME as plasticizer (spotted), and a different polymer matrix (checkered). The EIS data obtained at (a) 40 °C and (b) 80 °C were analyzed by Nyquist plot fitting (dark color) and distribution of relaxation times analysis (bright color) to extract R_{SEI}. The R_{SEI} values were divided by two to represent per-interface values.

26884062, 2026, 7, Downloaded from https://onlinelibrary.wiley.com/doi/10.1002/sstr.70532, Wiley Online Library on [17/11/2026]. See the Terms and Conditions (https://onlinelibrary.wiley.com/terms-and-conditions) on Wiley Online Library for rules of use; OA articles are governed by the applicable Creative Commons License

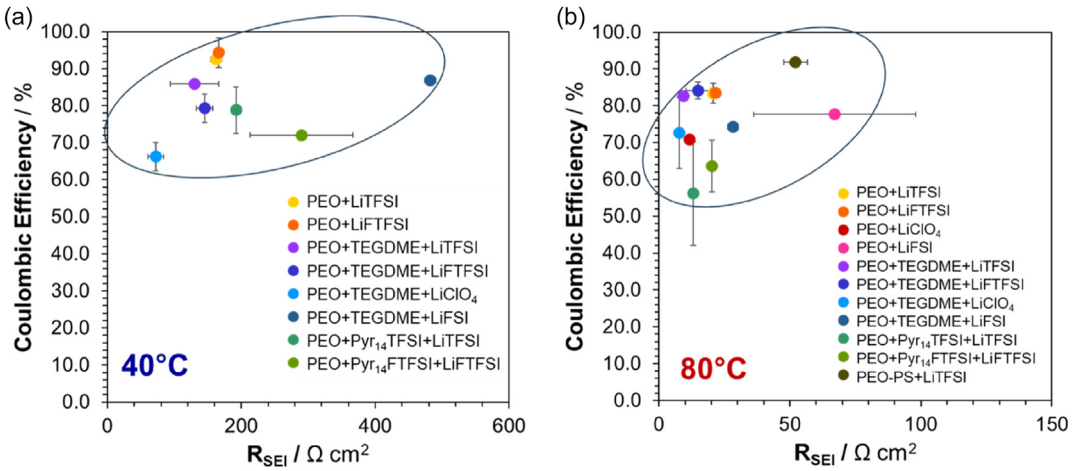


FIGURE 7 | Correlation of CE with the SEI resistance R_{SEI}. R_{SEI} values obtained from Nyquist plot fitting of EIS data at (a) 40 °C and (b) 80 °C for a set of PEO-based polymer electrolytes with different composition (see Figure 6) are plotted in relation to the respective average CEs determined in Cu ‖ Li cells. The PCC for these data points is 0.18 at 40 °C and 0.35 at 80 °C.

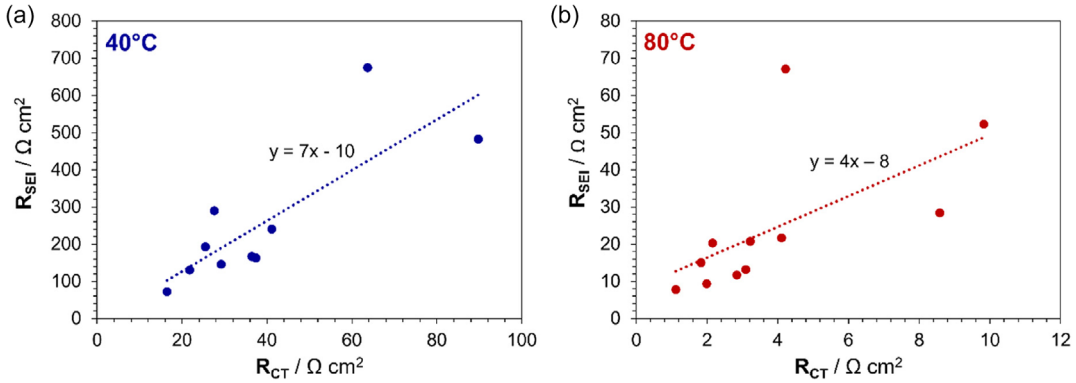


FIGURE 8 | Correlation between the charge transfer resistance R_{ct} and the SEI resistance R_{SEI}. Resistances were obtained from Nyquist plot fitting of the EIS data acquired at (a) 40 °C and (b) 80 °C in Li||Li cells.

3 | Conclusions

In this study, we systematically determined the exchange current densities for a broad set of PEO-based polymer electrolytes at the lithium|electrolyte interface using a validated and consistent methodology. By applying this uniform approach to electrolytes that differ in their polymer architecture, conducting salt, and plasticization, influencing factors and general trends have been identified. While the temperature exerted a strong influence on the interfacial kinetics, as expected, increasing j_0 by roughly an order of magnitude from 40 °C to 80 °C, the polymer matrix, conducting salt, and liquid content introduced additional variations. In particular, the addition of plasticizers led to increased j_0 values by enhancing mobility and wetting and/or altering the solvation environment, and salt-dependent trends reflected known coordination and desolvation chemistry. These results align very well with mechanistic expectations but also help to bridge the existing gap in the literature by providing a coherent and directly comparable dataset of j_0 values for diverse polymer electrolytes.

Building on these findings, we examined how the interfacial charge–transfer kinetics relate to the lithium plating/stripping reversibility by correlating both the charge–transfer resistance ($R_{ct} \sim 1/j_0$) and SEI resistance with the CEs measured after SEI formation. Across the range of compositions studied, we found that smaller j_0 values and larger R_{SEI} consistently coincide with a tendentially higher CE. This indicates that moderated interfacial kinetics – together with a sufficiently resistive, i.e., passivating and homogeneous interphase – can promote higher plating/stripping efficiencies in polymer electrolytes.

Overall, the results obtained in this study provide a coherent dataset of interfacial charge transfer kinetics for different polymer electrolytes, and shed light on their relation to the CE, highlighting the importance of deliberate electrolyte and interphase design to achieve a highly reversible lithium stripping and plating in polymer-based LMBs.

4 | Methods

The experimental procedures for the polymer electrolyte fabrication (Section 4.2), cell assembly (Section 4.3), and determination of the exchange current density j_0 by EIS and corresponding data analysis (Section 4.4) largely follow our previously reported protocol [7], with minor modifications as detailed below.

26884062, 2026, 7, Downloaded from https://onlinelibrary.wiley.com/doi/10.1002/sstr.70532, Wiley Online Library on [17/11/2026]. See the Terms and Conditions (https://onlinelibrary.wiley.com/terms-and-conditions) on Wiley Online Library for rules of use; OA articles are governed by the applicable Creative Commons License

4.1 | Ionic Liquid Preparation

Pyrrolidinium-based ionic liquids were synthesized according to the procedure reported by Montanino et al. [45]. The purified ionic liquids, $Pyr_{14}TFSI$ and $Pyr_{14}FTFSI$, were pre-dried under vacuum at 10^{-3} mbar (in the dry room), and then dried using a turbo molecular pump at 10^{-7} mbar and 20 °C for 2 h, then at 50 °C for 6 h and, finally, at 80 °C for 12 h. The ionic liquid electrolyte mixtures [$Pyr_{14}TFSI$:LiTFSI] and [$Pyr_{14}FTFSI$:LiFTFSI] were prepared in molar ratios of 8:2, and then dried again at 10^{-7} mbar and 80 °C for 12 h [46].

4.2 | Polymer Electrolyte Fabrication

Following Ref [7]., polymer electrolytes were prepared in a dry room (dew point ≈ −70 °C, corresponding to <2 ppm H_2O) by mixing polyethylene oxide (PEO, $M_W = 4$ Mio. g mol^{-1}, Sigma–Aldrich; dried at 50 °C for 48 h) with the respective conducting salt and benzophenone (≥99% purity, Merck), which served as UV cross-linking initiator. The mixing ratio of ethylene oxide: salt:benzophenone was 100:10:1 (by moles). The salts used are LiTFSI (3M), LiFSI (Provisco CS), LiFTFSI (Provisco CS), and $LiClO_4$ (Sigma–Aldrich), each dried under vacuum prior to use for at least 24 h: LiTFSI at 120 °C, LiFTFSI at 80 °C, LiFSI at 80 °C, and $LiClO_4$ at 120 °C. For the plasticized polymer electrolytes containing TEGDME (Sigma–Aldrich), half of the PEO mass was substituted with TEGDME. For the plasticized polymer electrolytes incorporating ionic liquids as plasticizers, one of the ionic liquids, [$Pyr_{14}TFSI$:LiTFSI] or [$Pyr_{14}FTFSI$:LiFTFSI], was added to PEO and benzophenone to yield a mixture with ethylene oxide: ionic liquid:salt:benzophenone molar ratio of 100:40:10:1. The precursors were mixed manually with a spatula in the specified ratios, sealed in pouch bags, and annealed at 65 °C for at least 24 h. The resulting materials were then hot-pressed up to 100 bar using a Polystat 200 T from Servitec with a thickness template to obtain membranes approximately 100 µm thick. Subsequently, the membranes were crosslinked twice for 6 min by exposing them to UV light in a UVACUBE 100 from Hönle UV Technology from both sides.

Polystyrene-*b*-poly(ethylene oxide) block copolymers (PS-PEO) were synthesized using anionic polymerization, as described in the literature [19]. The molecular weights of the PEO and PS blocks were 222 and 200 kg mol^{-1}, respectively. The PS-PEO was transferred to an argon-filled glovebox (MBraun), where the H_2O and O_2 levels were both maintained to be less than 0.1 ppm, and dried at 120 °C to remove any residual moisture. PS-PEO and LiTFSI were mixed in *N*-methyl-2-pyrrolidone and stirred at 100 °C until the lithium salt was fully dissolved. The mixing ratio of ethylene oxide and the lithium salt was 11.76:1 (by moles). The solution was poured onto a nickel foil on a casting plate and heated at 60 °C for 24 h. The semi-transparent film was peeled from the nickel foil and further dried at 120 °C in the glovebox antechamber under vacuum for 48 h. The films were placed in pouch material and sealed under vacuum prior to shipping to HIU.

4.3 | Cell Fabrication

For the determination of the exchange current density (j_0), symmetric Li||Li pouch cells were assembled with the polymer-based electrolyte membranes acting simultaneously as separator and electrolyte. For determining the CE, Cu||Li cells were employed. Lithium metal was purchased from Honjo Metal Co., and the electrodes had an area of approximately 1–2 cm^2. All cells were assembled in a dry room (dew point ≈ −70 °C ≡ <2 ppm H_2O). Squared polymer electrolyte membranes were cut and sandwiched between the overlapping lithium and copper or lithium electrodes connected to nickel tabs, which extended outside the pouch cell housing. The cells were vacuum-sealed and laminated using a GBC Fusion 1000L laminator prior to electrochemical testing.

4.4 | Electrochemical Testing and Data Analysis

To determine j_0 with the different polymer electrolytes, EIS was conducted on Li||Li cells at 40 °C and 80 °C. After equilibration at open-circuit voltage for 24 h, alternating voltages with an amplitude of 10 mV were applied over a frequency range from 1 MHz to 100 mHz to record the impedance response using a Solartron SI 1287 or a BioLogic VMP-3e.

To extract the charge transfer and the SEI resistances from the EIS data, the resulting Nyquist plots were fitted using the RelaxIS3 software from rhd instruments with an appropriate equivalent circuit model, as described in the literature [7]. For the plasticized electrolytes, an additional (R)(CPE) element was included to account for a minor feature observed at mid-to-low frequencies between the response from the (R_{SEI})(CPE) element and the low-frequency Warburg tail – possibly attributable to a charge layer. The DRT analysis was also performed using RelaxIS3 in the frequency range from 5 Hz to 1 MHz. The regularization parameter λ was set between 0.0001 and 0.01, guided by the approach described in Ref [47]. λ was gradually reduced until the sum of the squared residuals between the experimental data and the spectrum reconstructed from the DRT stabilized, ensuring an optimal trade-off between fitting accuracy and regularization. Peaks in the DRT spectra were fitted with Gaussian functions to quantify their area, corresponding to the respective resistance contributions.

For determining the CE with the different polymer electrolytes, Cu||Li cells were used, following the procedure described by Adams et al. [27]. After a 24 h rest period under open-circuit conditions, a certain amount of lithium ($Q_{conditioning} = 1.3$ mAh cm^{-2}) was plated and stripped (cut-off: 0.1 V) for SEI formation purposes. To determine the average CE during plating and stripping, next, a lithium reservoir of $Q_{reservoir} = 0.4$ mAh cm^{-2} was plated, followed by ten stripping/plating cycles at lower capacity ($Q_{cycle} = 30$ µAh cm^{-2}). A final stripping step up to 0.5 V depletes the lithium reservoir completely ($Q_{remaining} \leq 0.4$ mAh cm^{-2}). All steps were performed at a current density of 0.02 mA cm^{-2}. The average CE can be calculated according to Equation (3):

$$\overline{CE} = \frac{10 * Q_{cycle} + Q_{remaining}}{10 * Q_{cycle} + Q_{reservoir}} \quad (3)$$

Author Contributions

The collaboration was initiated by Y.S.-H. and D.B.. K.G. designed the study, performed the experiments, and drafted the manuscript under the supervision of D.B., building on prior joint work with B.T. J.E.-A.

26884062, 2026, 7, Downloaded from https://onlinelibrary.wiley.com/doi/10.1002/sstr.70532, Wiley Online Library on [17/11/2026]. See the Terms and Conditions (https://onlinelibrary.wiley.com/terms-and-conditions) on Wiley Online Library for rules of use; OA articles are governed by the applicable Creative Commons License

consulted on the manuscript's structure, S.P. on study design and data interpretation. Z.L. and V.P. prepared some materials for this study. All authors reviewed and edited the manuscript.

Acknowledgments

This work was funded by the US-German collaboration on "Interfaces and Interphases in Rechargeable Li-metal based Batteries" in the frame of the joint research project "LISI(−2)" by the German Federal Ministry of Research, Technology and Space (BMFTR; 03XP0224D and 03XP0509D) and the U.S. Department of Energy under the Advanced Battery Materials Research Program (BMR; DOE; DE-AC02-05CH11231 and DE-AC02-06CH11357). K. G., J. C. E.-A., Z. L, and D. B. would additionally like to acknowledge financial support from the Helmholtz Association and Y. S.-H. and B. T. from the NASA Ames Research Center, award number 80NSSC21M0108. K. G. is moreover grateful for funding from the Studienstiftung des deutschen Volkes.

Funding

This work was supported by the Bundesministerium für Bildung und Forschung (03XP0224D and 03XP0509D), U.S. Department of Energy (DE-AC02-05CH11231 and DE-AC02-06CH11357), Ames Research Center (80NSSC21M0108).

Conflicts of Interest

The authors declare no conflicts of interest.

Data Availability Statement

The datasets generated during and/or analyzed during the current study are available from the corresponding author upon reasonable request.

References

1. Z. Song, F. Chen, M. Martinez-Ibañez, et al., "A Reflection on Polymer Electrolytes for Solid-State Lithium Metal Batteries," *Nature Communications* 14 (2023): 4884.

2. D. Bresser, S. Lyonnard, C. Iojoiu, L. Picard, and S. Passerini, "Decoupling Segmental Relaxation and Ionic Conductivity for Lithium-Ion Polymer Electrolytes," *Molecular Systems Design & Engineering* 4 (2019): 779.

3. Y. Liu, X. Xu, M. Sadd, et al., "Insight into the Critical Role of Exchange Current Density on Electrodeposition Behavior of Lithium Metal," *Advanced Science* 8 (2021): 2003301.

4. G. M. Hobold, J. Lopez, R. Guo, et al., "Moving beyond 99.9% Coulombic Efficiency for Lithium Anodes in Liquid Electrolytes," *Nature Energy* 6 (2021): 951.

5. C. O. Plaza-Rivera, D. Wang, J. K. Phong, et al., "Concentration-Dependent Thermodynamics and Kinetics in Lithium-Metal Battery Electrolytes: Implications for Coulombic Efficiency," *ACS Energy Letters* 10 (2025): 3025.

6. G. M. Hobold, K.-H. Kim, and B. M. Gallant, "Beneficial *vs*. Inhibiting Passivation by the Native Lithium Solid Electrolyte Interphase Revealed by Electrochemical Li^+ Exchange," *Energy & Environmental Science* 16 (2023): 2247.

7. K. Geng, B. A. Tappan, S. Passerini, Y. Shao-Horn, and D. Bresser, "Determination of the Exchange Current Density at Lithium | Polymer Electrolyte Interfaces," *Advanced Science* 13 (2025): e14492.

8. L. Blume, U. Sauter, and T. Jacob, "Non-Linear Kinetics of the Lithium-Solid Polymer Electrolyte Interface," *Electrochimica Acta* 318 (2019): 551.

9. B. A. Tappan, K. Geng, D. Vivona, et al., "Investigation of Charge Transfer Kinetics in Multilayer PEO/LLZO Solid-State Batteries," *ACS Applied Materials & Interfaces* 17 (2025): 18255.

10. M. Egashira, Y. Utsunomiya, N. Yoshimoto, and M. Morita, "Effects of the Surface Treatment of the Al_2O_3 Filler on the Lithium Electrode/Solid Polymer Electrolyte Interface Properties," *Electrochimica Acta* 52 (2006): 1082.

11. J. A. Isaac, L. R. Mangani, D. Devaux, and R. Bouchet, "Electrochemical Impedance Spectroscopy of PEO-LATP Model Multilayers: Ionic Charge Transport and Transfer," *ACS Applied Materials & Interfaces* 14 (2022): 13158.

12. D. Fauteux, "Lithium Electrode/PEO-Based Polymer Electrolyte Interface Behavior Between 60° and 120°C," *Journal of the Electrochemical Society* 135 (1988): 2231.

13. P. Senthil Kumar, A. Sakunthala, M. V. Reddy, and M. Prabu, "Structural, Morphological, Electrical and Electrochemical Study on Plasticized PVdF-HFP/PEMA Blended Polymer Electrolyte for Lithium Polymer Battery Application," *Solid State Ionics* 319 (2018): 256.

14. M. Forsyth, P. Meakin, D. R. MacFarlane, and A. J. Hill, "Free Volume and Conductivity of Plasticized Polyether-urethane Solid Polymer Electrolytes," *Journal of Physics: Condensed Matter* 7 (1995): 7601.

15. Y. Zhao and W. E. Tenhaeff, "Thermally and Oxidatively Stable Polymer Electrolyte for Lithium Batteries Enabled by Phthalate Plasticization," *ACS Applied Polymer Materials* 2 (2020): 80.

16. X. Jiang, J. Chen, J. Zeng, et al., "Decoupling Li^+ Conductivity and Mechanical Stability in a Thermally Reversible Concentrated Sulfone-Based Gel Electrolyte for Lithium Metal Batteries," *Journal of Materials Chemistry A* 12 (2024): 21912.

17. M. Kumar and S. S. Sekhon, "Role of Plasticizer's Dielectric Constant on Conductivity Modification of PEO–NH_4F Polymer Electrolytes," *European Polymer Journal* 38 (2002): 1297.

18. T. Zhou, Y. Zhao, J. W. Choi, and A. Coskun, "Ionic Liquid Functionalized Gel Polymer Electrolytes for Stable Lithium Metal Batteries," *Angewandte Chemie International Edition* 60 (2021): 22791.

19. J. A. Maslyn, W. S. Loo, K. D. McEntush, et al., "Growth of Lithium Dendrites and Globules through a Solid Block Copolymer Electrolyte as a Function of Current Density," *Journal of Physical Chemistry C* 122 (2018): 26797.

20. K. L. Browning, R. L. Sacci, and G. M. Veith, "Energetics of Na^+ Transport through the Electrode/Cathode Interface in Single Solvent Electrolytes," *Journal of the Electrochemical Society* 164 (2017): A580.

21. F. Sagane and T. Suzuki, "The Influence of the Coordination on the Kinetic Behavior of the Anion Intercalation/De-Intercalation into the Graphite Electrode," *Journal of the Electrochemical Society* 169 (2022): 100505.

22. Y. Pan, H. Yu, Y. Zhang, et al., "In-Depth Exploration of the Effect Mechanisms of Various Lithium Salt Anions in Solid-State and Liquid Lithium Metal Batteries," *Journal of Materials Chemistry A* 12 (2024): 16447.

23. J. Holoubek, K. Yu, J. Wu, et al., "Toward a Quantitative Interfacial Description of Solvation for Li Metal Battery Operation under Extreme Conditions," *Proceedings of the National Academy of Sciences of the United States of America* 120 (2023): e2310714120, https://doi.org/10.1073/pnas.2310714120.

24. M. Wetjen, G.-T. Kim, M. Joost, M. Winter, and S. Passerini, "Temperature Dependence of Electrochemical Properties of Cross-Linked Poly(ethylene Oxide)–lithium Bis(trifluoromethanesulfonyl) imide–N-Butyl-N-Methylpyrrolidinium Bis(trifluoromethanesulfonyl) imide Solid Polymer Electrolytes for Lithium Batteries," *Electrochimica Acta* 87 (2013): 779.

25. G. B. Appetecchi, G.-T. Kim, M. Montanino, et al., "Ternary Polymer Electrolytes Containing Pyrrolidinium-Based Polymeric Ionic Liquids for Lithium Batteries," *Journal of Power Sources* 195 (2010): 3668.

26. N. Munichandraiah, L. G. Scanlon, and R. A. Marsh, "Surface Films of Lithium: An Overview of Electrochemical Studies," *Journal of Power Sources* 72 (1998): 203.

26884062, 2026, 7, Downloaded from https://onlinelibrary.wiley.com/doi/10.1002/sstr.70532, Wiley Online Library on [17/11/2026]. See the Terms and Conditions (https://onlinelibrary.wiley.com/terms-and-conditions) on Wiley Online Library for rules of use; OA articles are governed by the applicable Creative Commons License

27. B. D. Adams, J. Zheng, X. Ren, W. Xu, and J. Zhang, "Accurate Determination of Coulombic Efficiency for Lithium Metal Anodes and Lithium Metal Batteries," *Advanced Energy Materials* 8 (2018): 1702097.

28. H. Zhang, C. Liu, L. Zheng, et al., "Lithium Bis(fluorosulfonyl)imide/Poly(ethylene Oxide) Polymer Electrolyte," *Electrochimica Acta* 133 (2014): 529.

29. R. Tanaka, M. Sakurai, H. Sekiguchi, and M. Inoue, "Improvement of Room-Temperature Conductivity and Thermal Stability of PEO–$LiClO_4$ Systems by Addition of a Small Proportion of Polyethylenimine," *Electrochimica Acta* 48 (2003): 2311.

30. J. A. Maslyn, L. Frenck, V. D. Veeraraghavan, et al., "Limiting Current in Nanostructured Block Copolymer Electrolytes," *Macromolecules* 54 (2021): 4010.

31. F. González, V. Gregorio, A. Rubio, L. Garrido, N. García, and P. Tiemblo, "Ionic Liquid-Based Thermoplastic Solid Electrolytes Processed by Solvent-Free Procedures," *Polymers* 10 (2018): 124.

32. K. Zhang, Y. Ji, Q. Wu, S. A. Nabavizadeh, Y. Qi, and L.-Q. Chen, "Simulating Solid Electrolyte Interphase Formation Spanning 10^8 Time Scales with an Atomically Informed Phase-field Model,"*Energy & Environmental Science* 18 (2025): 7541–7554, https://doi.org/10.1039/d5ee01030f.

33. S. Patra, P. Thakur, B. Soman, et al., "Mechanistic Insight into the Improved Li Ion Conductivity of Solid Polymer Electrolytes," *RSC Advances* 9 (2019): 38646.

34. W. Qin, Q. Yang, Y. He, L. Zhang, and H. Hu, "Finite Elastic-Viscoplastic Deformation Behaviour of PEO-Based Solid Polymer Electrolyte: Experimental Investigation and Constitutive Modelling," *Mechanics of Materials* 185 (2023): 104773.

35. K. Geng, "Charge Transfer and Transport at Lithium | Polymer Electrolyte Interfaces" (Karlsruher Institut für Technologie (KIT), 2026), https://publikationen.bibliothek.kit.edu/1000190951.

36. C. Monroe and J. Newman, "The Impact of Elastic Deformation on Deposition Kinetics at Lithium/Polymer Interfaces," *Journal of the Electrochemical Society* 152 (2005): A396.

37. M. Singh, O. Odusanya, G. M. Wilmes, et al., "Effect of Molecular Weight on the Mechanical and Electrical Properties of Block Copolymer Electrolytes," *Macromolecules* 40 (2007): 4578.

38. C. Su, M. He, J. Shi, R. Amine, J. Zhang, and K. Amine, "Solvation Rule for Solid-Electrolyte Interphase Enabler in Lithium-Metal Batteries," *Angewandte Chemie International Edition* 59 (2020): 18229.

39. B. Horstmann, J. Shi, R. Amine, et al., "Strategies towards Enabling Lithium Metal in Batteries: Interphases and Electrodes," *Energy & Environmental Science* 14 (2021): 5289.

40. L. Stolz, G. Homann, M. Winter, and J. Kasnatscheew, "The Sand Equation and Its Enormous Practical Relevance for Solid-State Lithium Metal Batteries," *Materials Today* 44 (2021): 9.

41. P. Lennartz, B. A. Paren, A. Herzog-Arbeitman, et al., "Practical Considerations for Enabling Li|polymer Electrolyte Batteries," *Joule* 7 (2023): 1471.

42. J. Liu, Z. Bao, Y. Cui, et al., "Pathways for Practical High-Energy Long-Cycling Lithium Metal Batteries," *Nature Energy* 4 (2019): 180.

43. X. Chen, Y. Yao, C. Yan, R. Zhang, X. Cheng, and Q. Zhang, "A Diffusion--Reaction Competition Mechanism to Tailor Lithium Deposition for Lithium-Metal Batteries," *Angewandte Chemie International Edition* 59 (2020): 7743.

44. P. Röring, J. Pleie, A. J. Butzelaar, et al., "A Critical Evaluation of the Limiting Current Density in Polymer Electrolytes: Interplay of Ion Transport, Mechanical Stability, and Conformal Li–Electrolyte Interfaces," *Journal of the American Chemical Society* 148 (2026): 4176.

45. M. Montanino, F. Alessandrini, S. Passerini, and G. B. Appetecchi, "Water-Based Synthesis of Hydrophobic Ionic Liquids for High-Energy Electrochemical Devices," *Electrochimica Acta* 96 (2013): 124.

46. D. Stępień, B. Wolff, T. Diemant, et al., "Insights into the Lithium Nucleation and Plating/Stripping Behavior in Ionic Liquid-Based Electrolytes," *ACS Applied Materials & Interfaces* 15 (2023): 25462.

47. M. Braig and R. Zeis, "Distribution of Relaxation Times Analysis of Electrochemical Hydrogen Pump Impedance Spectra," *Journal of Power Sources* 576 (2023): 233203.

Supporting Information

Additional supporting information can be found online in the Supporting Information section.

26884062, 2026, 7, Downloaded from https://onlinelibrary.wiley.com/doi/10.1002/sstr.70532, Wiley Online Library on [17/11/2026]. See the Terms and Conditions (https://onlinelibrary.wiley.com/terms-and-conditions) on Wiley Online Library for rules of use; OA articles are governed by the applicable Creative Commons License